

Studies on conductivity, morphology and thermal stability of PMMA-PSAN based Solid Polymer Electrolytes using SiO₂ as nanofiller

S. V. Ganesan^{1*}, K. K. Mothilal^{1*}, S. Selvasekarapandian², T. K. Ganesan³.

¹Department of Chemistry, Saraswathi Narayanan College, Madurai - 625 022, India.

²Materials Research Center, Ramanathapuram, Coimbatore -641 045, India.

³Department of Chemistry, The American College, Madurai – 625 002, India.

Abstract : The solid polymer electrolyte (SPE) involving fixed concentration of Poly(methyl methacrylate) (PMMA) and Poly(styrene-co-acrylonitrile) (PSAN) as host polymers with Ethylene carbonate (EC), Propylene carbonate (PC) as plasticizers, Lithium trifluoro methanesulfonate (LiCF₃SO₃) as salt and varying concentration of SiO₂ as nano-filler were prepared by solution casting technique. The prepared samples were labelled as S0, S1, S2, S3, S4, S5 corresponding to SiO₂ nano-filler concentration of 0, 5, 6, 7, 8, 9 in wt%. The functional group interaction and structural reorganisation of SPE S0, S2 and S5 were studied by Fourier transform infrared (FT-IR) technique. X-ray diffraction (XRD) technique is used to study the crystallinity of the SPE S2 and compared with PMMA, PSAN and sample S0. The AC impedance spectroscopy is used to study the ionic conductivity of the prepared samples. Sample S2 shows a maximum conductivity of $6.55 \times 10^{-5} \text{ S cm}^{-1}$ at 70 °C. The temperature dependence of conductivity of the films seems to obey VTF relation. Thermal analysis of the sample S2 was done using Thermo-gravimetric analysis (TGA) and Differential scanning calorimetry (DSC) techniques. TG and derivative TG analysis show thermal stability of the sample S2 up to 278 °C. Glass Transition Temperature (T_g) of sample S2 is compared with pure PMMA, pure PSAN, and sample S0. The morphology of the sample S2 is compared with sample S5 using Scanning electron microscopy (SEM) Analysis. It is found that the nanofiller SiO₂ provides extra conduction channels leading to enhanced conductivity in sample S2 which is not observed in S5.

Key words : SPE, FT-IR, XRD, AC impedance, TGA, DSC, SEM.

Introduction

Polymer electrolytes play a key role in modern energy technology. Since the first report by Armand et.al, on polymer electrolytes in 1979, focus on the development of secondary rechargeable lithium ion batteries involving polymer electrolytes have been the emerging area of research interest ⁽¹⁾. In order to enhance the conductivity and stability of polymer electrolytes, several combinations of approaches like copolymerisation, blending, plasticization and addition of fillers are carried out ⁽²⁾. By changing the composition of blend matrix, polymer blends are known to exhibit superior properties when compared to individual polymer electrolytes. Usually, one phase of the polymer blend is involved in absorption of electroactive species, while the other phase being tougher and substantially inert contributes to the thermal and mechanical stability of the blend polymer electrolyte film ⁽³⁾. However, low conductivity of the solid polymer electrolytes and poor mechanical integrity of the gelled polymer electrolytes have been the driving force towards focus on the composite solid polymer

electrolytes that allows fabrication of flexible thin film of desired shape ⁽⁴⁾. In order to improve ionic conductivity, plasticizers are incorporated into the solid polymer blend matrix. Carbonate based plasticizers like ethylene carbonate and propylene carbonate helps in the solvation of Li⁺ ion. It reduces glass transition temperature of the polymer blends leading to increase in the segmental motion of the polymer chains thus enhancing conductivity ⁽⁵⁾. The use of plasticizers with high dielectric constant results in better dissociation of lithium salt, leading to increase in the number of free mobile charge carriers thus enhances conductivity ⁽⁶⁾. The incorporation of nano-sized fillers like SiO₂ increases mechanical strength, thermal stability of the solid polymer electrolyte ⁽⁷⁾. It also increases ionic conductivity by reducing crystallinity of the polymer blend ⁽⁸⁾. The mobile charge carriers are known to interact with the O²⁻/OH groups of the fillers in a Lewis acid- base type leading to enhanced ionic transportation between the electrodes.

So far there are no reports to the best of our knowledge involving blending of two amorphous polymers for preparation of polymer electrolytes. In literature, there are very few works in which amorphous polymer poly(styrene-co-acrylonitrile) is usually blend with either semi-crystalline polymers like poly(vinylidene fluoride-co-hexafluoropropylene) (PVdF-HFP) or crystalline polymers like poly(vinylidene fluoride) (PVdF). Therefore, we choose two amorphous polymers PMMA and PSAN to form polymer blend host system. In this study, the polymer compositions poly(methyl methacrylate) (25) – poly(styrene-co-acrylonitrile) (25) in weight percentage to the whole system was chosen, as G.N. Kumaraswamy et al., ⁽⁹⁾ and Miao D et al., ⁽¹⁰⁾ have described that the miscibility window exists for 10-30 wt% of PMMA in PMMA/PSAN blend system. Beyond 30 wt%, though the blend system is miscible yet, the hydrodynamic parameters and phase separation temperatures seems to decrease suggesting immiscibility at higher temperatures (above 160 °C). Except for the miscibility studies stated above, so far there are no reports in the literature involving the conductivity studies of polymer electrolytes comprising PMMA and PSAN polymer blends. K.W. Chew et al., ⁽¹¹⁾ have described more effectiveness of the polymer electrolyte involving PMMA and LiCF₃SO₃ compared to PMMA and LiBF₄ in terms of higher room temperature conductivity values. Moreover, Lithium triflate is chosen for this study as it is a nontoxic, thermally stable salt that is miscible with organic solvents particularly THF. The plasticizers ethylene carbonate and propylene carbonate are chosen for this study. Since they possess high dielectric constant and are known to solvate Li⁺ ions more effectively. Solvent THF is chosen for its efficacy in dissolving polymers, high volatility and excellent film forming ability ⁽¹²⁾. The nano-filler SiO₂ (10 -20 nm) is chosen for this study as it is an inert inorganic filler providing large amount of surface area for interaction. Therefore, an attempt has been made to study the effect of various concentration of nanosized filler SiO₂ on the conductivity, morphology and thermal stability of the composite solid polymer blend system comprising of PMMA, PSAN, EC, PC and Lithium triflate. The above system is subjected to FT-IR, XRD, AC impedance, SEM, TGA and DSC studies for complexation, conductivity, morphology and thermal stability.

Experimental Section

Sample Preparation

All the samples were prepared by solution casting technique ⁽¹³⁾. The polymers poly(methyl methacrylate) (PMMA, Avg. M_w = 5.5 x 10⁵) was purchased from Alfa-aesar and poly(styrene-co-acrylonitrile) (PSAN, Avg. M_w = 1.65 x 10⁵) was purchased from Sigma-Aldrich and dried at 100 °C in vacuum for 10 h before use. The plasticizers, ethylene carbonate (99%) and propylene carbonate (99%) were purchased from Alfa-aesar and used as such. The Lithium triflate salt with 99.995% purity was purchased from Sigma-Aldrich and used as such. The inorganic nano filler SiO₂ 99.95% (~10-20 nm) was purchased from Sigma-Aldrich and dried in vacuum at 100 °C before use. The solvent THF with 99.9% purity was purchased from SRL and used as such.

In a separate conical flask, the polymers PMMA (25 wt%) and PSAN (25 wt%) were blended in tetrahydrofuran solvent. The lithium triflate (20 wt %) was blend with plasticizers ethylene carbonate and propylene carbonate in tetrahydrofuran solvent in another conical flask and transferred to the conical flask containing polymer blends, stirred well for few hours at room temperature. Varying concentration (wt%) of nano-filler SiO₂ (10-20 nm) in the range of 0, 5, 6, 7, 8, 9 were added to the above system and stirred for ~24 h at room temperature and at 60 °C for few hours before casting the solution onto a teflon coated glass plate. The solvent tetrahydrofuran was allowed to evaporate slowly at room temperature for 24 h until then the polymer electrolyte film is formed. Now, the traces of the solvent were evaporated by drying at 70 °C in vacuum for 10

h. The solid polymer electrolytes obtained were absolutely dry, opaque, flexible thin films resembling a plastic sheet of paper. The prepared samples were labelled as S0, S1, S2, S3, S4, S5 corresponding to SiO₂ nano-filler concentration of 0, 5, 6, 7, 8, 9 in wt%. The SPE samples were then transferred into dessicator and stored till use in experiments.

Measurements

The XRD equipment X' Pert pro PANalytical X-ray diffractometer was used for powder XRD studies. The Fourier transform infrared spectra (Shimadzu FTIR8400S) of the samples were recorded in the range 4000 – 500 cm⁻¹. The ac impedance measurements were carried out using HIOKI 3532 -50 LCR Hi TESTER over a frequency range of 42 Hz – 1MHz in the temperature range of 303 - 373 K. The intercept on the real axis (upon extrapolation) obtained from cole-cole plot gives the bulk electrolyte resistance (R_b). The ionic conductivity (σ) is calculated from the measured bulk resistance (R_b) for the known area of the polymer electrolyte film with known thickness using the formula:

$$\sigma (\text{Scm}^{-1}) = (L/A) \times 1/R_b \quad \text{where } L = \text{thickness of the SPE film, } A = \text{area of contact.}$$

The thermal analysis (TG/DTG) was performed for the sample with highest conductivity using TA Instrument SDT Q600 V20.9 Build 20 at a heating rate of 10 °C per minute from room temperature to 700 °C in nitrogen atmosphere. DSC analysis was carried out using TA Instrument DSC Q20 V24.10 Build 122 analyzer in the temperature range 0 °C to 250 °C at a heating rate of 10 °C per minute in nitrogen atmosphere. SEM analysis is carried out using VEGA3 TESCAN instrument to study the surface morphology of the samples.

Results and Discussion

XRD Studies

The X-ray diffraction measurements are carried out to study the crystalline nature and complexation behaviour of samples S0, S2 and compare it with individual polymer poly (methylmethacrylate), poly (styrene-co-acrylonitrile). It is evident from figure 1 that both S0 and S2 are amorphous in nature. Pure PMMA and PSAN also exhibit amorphous nature. The presence of broad bands with no definite crystalline peaks shows amorphous behaviour⁽¹⁴⁾. The S0 and S2 show no peaks corresponding to lithium triflate in the sample. The absence of these peaks in the solid polymer electrolyte sample S2 containing nano filler SiO₂ shows complete dissolution of the salt and filler in the plasticizer rich polymer blend electrolyte medium⁽¹⁵⁾.

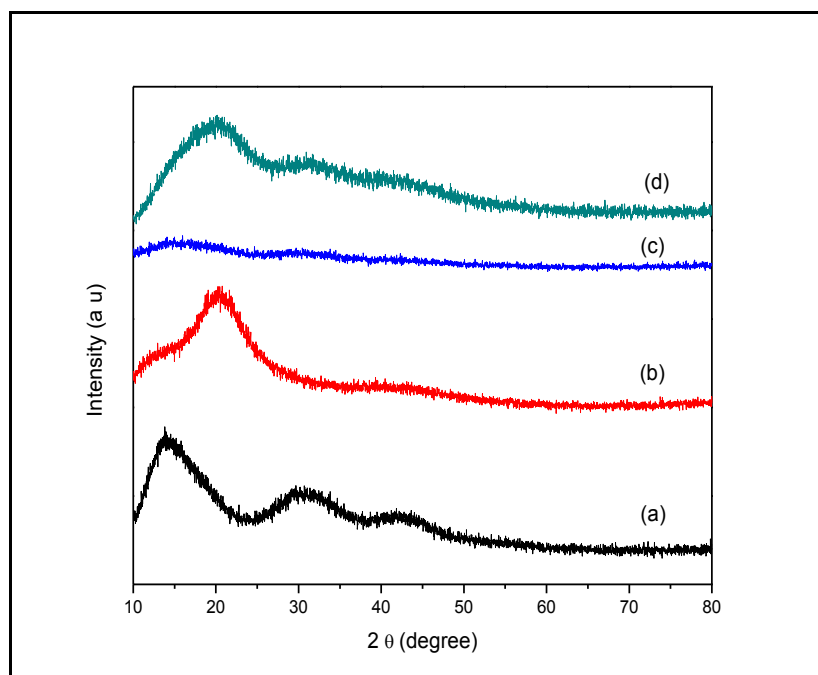


Figure 1: XRD pattern of (a) pure PMMA, (b) pure PSAN, (c) SPE (S0) (d) SPE (S2).

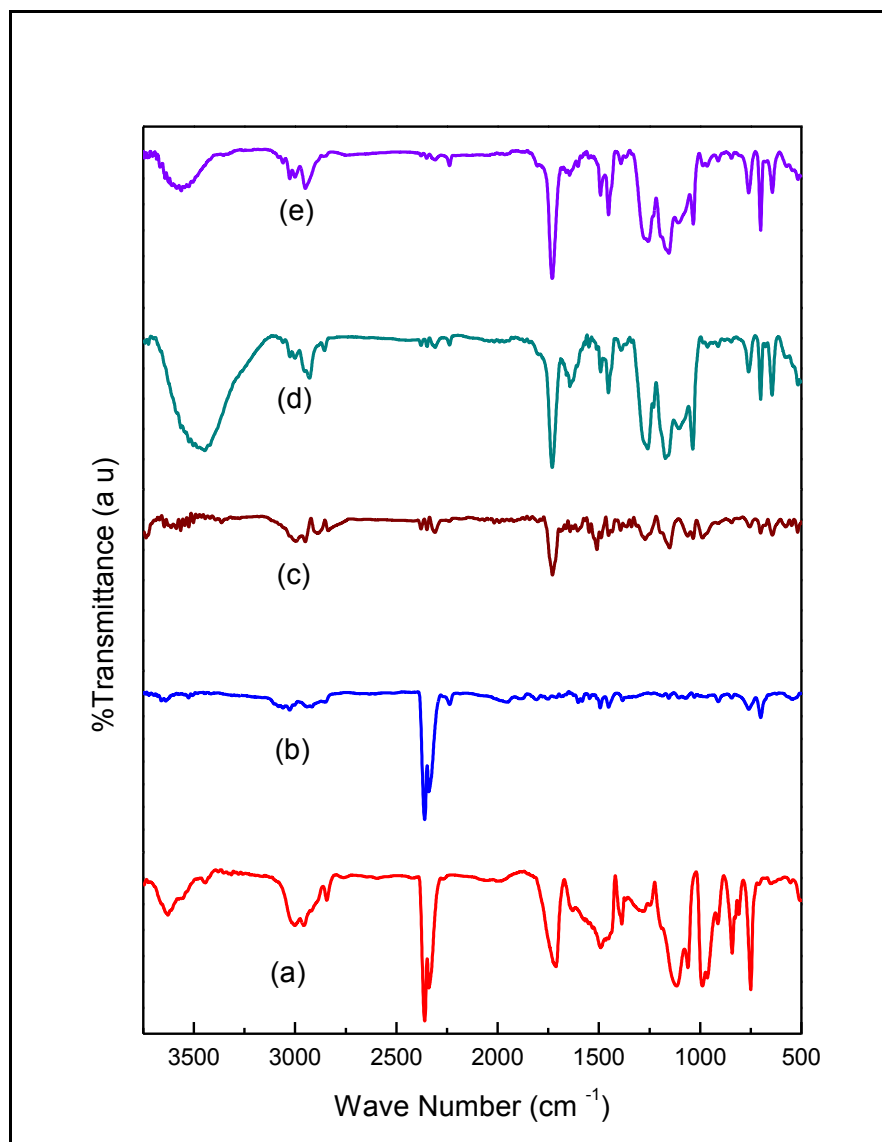


Figure 2: FT-IR spectra of (a) PMMA (b) PSAN (c) SPE (S0) (d) SPE (S2) (e) SPE (S5)

FT-IR Studies

From Table 1 & Figure 2, the IR vibrational frequencies at 846, 983, 1170 cm^{-1} for S2 and at 845, 971, 1154 cm^{-1} for S5 correspond to CH_2 rocking, wagging, twisting vibrations respectively. The rocking and twisting vibrational frequencies are at higher values compared to PMMA (841 & 1116 cm^{-1}) as it involves C-O-C bending and stretching vibrations also⁽¹⁵⁾. The decrease in values for wagging vibration of samples S2 and S5 compared to PMMA (988 cm^{-1}), suggests CH_2 groups and C-O-C groups are involved in interaction with lithium triflate salt and the nano-filler SiO_2 ⁽¹⁶⁾.

Table 1: Assignment of FT-IR vibrational frequencies of the polymers and the complexes.

PMMA	PSAN	S0	S2	S5	Functional group vibration
841.8		841.8	846	845	C-O-C bending, CH_2 rocking
988		988	983	971	CH_2 wagging
1116.7		1150	1170.7	1154	CH_2 Twisting, C-O-C stretching
1386.7		1389	1387	1388	O- CH_3 deformation
	1452	1452	1453	1452	C=C ring stretching
1498		1487	1485	1482	O- CH_3 stretching

1060		1034	1036.6	1033.7	C-O stretch,
1278.7		1271	1259	1256.5	C-C-O stretching
	2239	2238	2238	2238	C≡N Stretching
1710.7		1729	1730	1732	C=O stretching
		1638	1638	1646	OH bending
2956.6	2918	2945	2929.6	2949.9	CH ₃ Stretching symmetric
3002		3000	2998	2999	CH ₃ Stretching asymmetric
	3027	3027	3026	3026	aromatic C-H stretching

Though there is not much change in the deformation frequency with respect to $-\text{OCH}_3$ group in both SPE's (S0, S2, S5) and the PMMA (1388 cm^{-1}), yet there occurs considerable decrease in $-\text{OCH}_3$ stretching frequency in SPE's (1485 cm^{-1}) compared to PMMA (1498 cm^{-1}). This shows Li^+ ion interacts with OCH_3 group⁽¹⁷⁾. The IR vibrational frequencies at $1034, 1271\text{ cm}^{-1}$ for S0, $1036, 1259\text{ cm}^{-1}$ for S2 and at $1033, 1256\text{ cm}^{-1}$ for S5 correspond to C-O, C-C-O stretching vibrations. The C-O and C-C-O stretching vibrations of S5 occur at lower value compared to S2 and PMMA ($1060, 1278\text{ cm}^{-1}$). This indicates that the Lithium salt interacts strongly with S5 than S2. Thus Lithium ion is considerably free in S2 because of the interaction with filler SiO_2 . The C=O stretching frequency of S0, S2 and S5 shows around 1730 cm^{-1} compared to 1710 cm^{-1} for PMMA. The increase may be due to presence of plasticizers ethylene carbonate and propylene carbonate which also contribute to C=O stretching frequency⁽¹⁸⁾. There is no change in the C≡N stretching frequency (2238 cm^{-1}) for both SPE's and PSAN. This indicates C≡N group does not interact with either Lithium salt or nanofiller SiO_2 . There is no change in the aromatic ring C-H stretching vibrations observed at 3026 cm^{-1} for SPE's (S0, S2, S5) and PSAN. This inferred that the aromatic ring is not involved in interaction with either the filler or Lithium salt. The IR vibrational stretching frequencies at $\sim 2950\text{ cm}^{-1}$ indicates the presence of CH_3 , CH_2 and CH groups in both the polymers and SPE's S0, S2, S5⁽¹⁹⁾.

IONIC Conductivity Studies

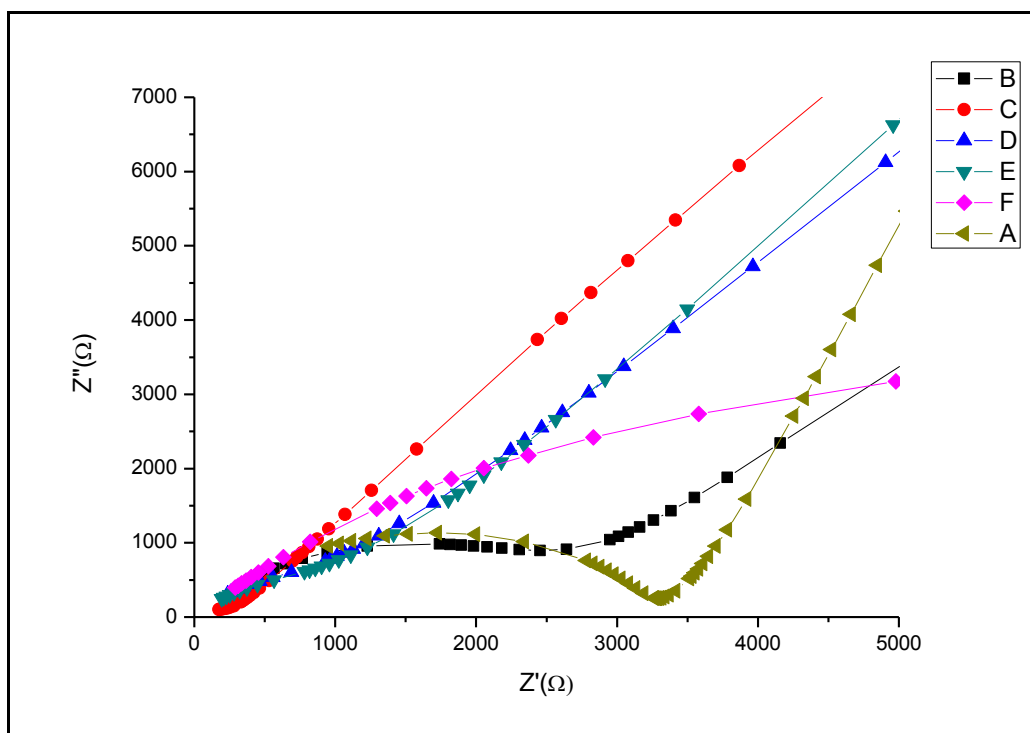


Figure 3a: Impedance plot of SPE's: PMMA-PSAN-EC-PC-LiCF₃SO₃-xSiO₂; were x= 0 wt% (A), 5 wt% (B), 6 wt% (C), 7 wt% (D), 8 wt% (E), 9 wt% (F).

Impedance spectroscopy is used to study the conductivity of polymer electrolyte films. Figure 3(a) shows complex AC impedance spectra of SPE samples (S0 – S5) at room temperature. From the figure, it is

inferred that in the absence of nano-filler SiO₂ there occurs a well defined semicircle before a slanting straight line for sample S0. The same seems to decrease as the concentration of nano-filler SiO₂ increases from 5 to 6 wt%. Further increase in concentration of the nano-filler SiO₂ exhibits either absence or very small negligible semi-circle with almost a straight line slanting to the Y axis. This observation in the Cole-Cole plot (Figure 3a) confirms that the addition of nano-filler SiO₂ leads to ion conduction as the only mechanism explaining the conductivity of the polymer electrolyte⁽²⁰⁾. The slanted spikes are attributed to the formation of double layer at the blocking electrodes leading to electrolyte resistance⁽²¹⁾.

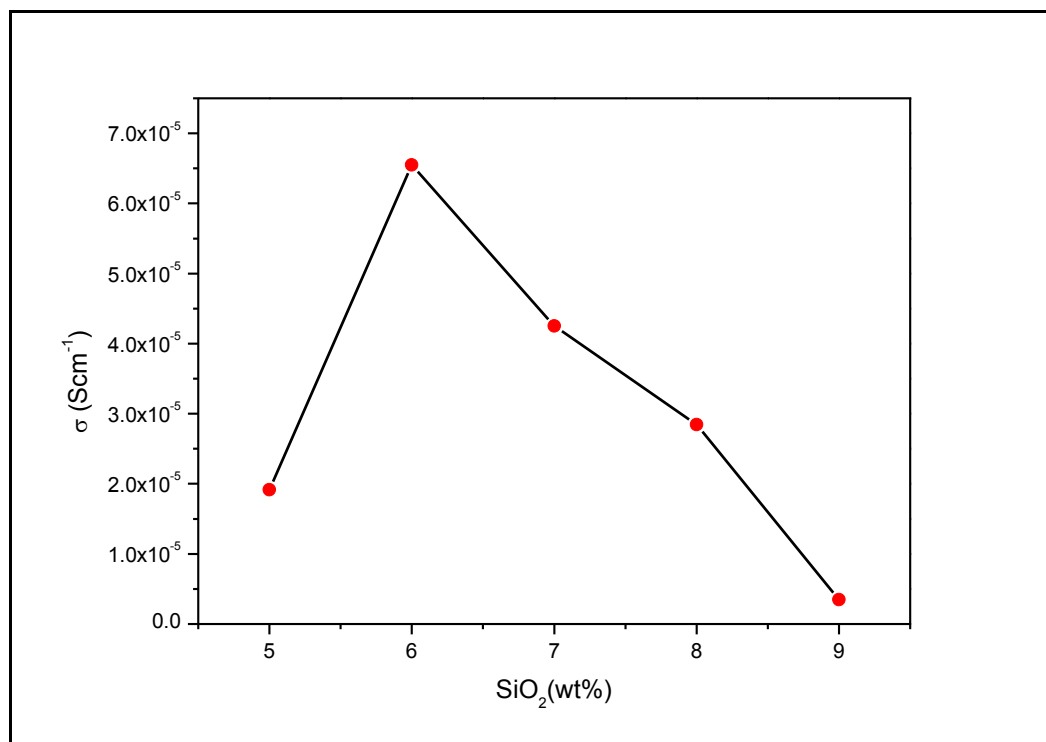


Figure 3.b: Variation of conductivity as a function of weight percentage of nano filler SiO₂ in SPE (S1 – S5) at 70 °C.

From the Cole-Cole plot (Figure 3a) and Figure (3b), the ionic conductivity increases with increase in the concentration of nano-filler SiO₂ content upto 6 wt%. The highest ionic conductivity value observed is $6.55 \times 10^{-5} \text{ Scm}^{-1}$ at 70 °C for 6 wt% of nano-filler SiO₂. The enhancement of ionic conductivity is due to interaction of the filler with either the anion or cation thereby reducing ion pairing and increasing the charge carrier density⁽²²⁾. The Lewis acid-base interaction between the filler surface groups and the polymer chain backbone also contributes to enhancement of conductivity. Hyung-Sun Kim et al.⁽²³⁾ reported that addition of SiO₂ reduces the glass transition temperature (T_g) and allows the amorphous polymer to provide specific liquid-like characteristics. By reducing the crystallization tendency, the amorphous phase or less ordered region gains more flexibility leading to increased segmental motion of the polymer blend chains thus enhancing ionic conductivity. Further, increase in the concentration of nanofiller SiO₂ leads to decrease in the ionic conductivity. This may be due to the formation of well defined crystallite regions due to increased abundance of the filler. It also leads to immobilisation of the polymer chain segments⁽²⁴⁾.

Temperature dependence of ionic conductivity

Variation of conductivity with increase in temperature (30 – 70 °C) of the solid polymer electrolyte samples (S0 –S5) is presented in Table 2. It is obvious from the Table 2 that the ionic conductivity of all samples increases with increase in temperature. This phenomenon is due to volume expansion of the polymer blend matrix with rise in temperature. From Figure 3(c), variation of conductivity of the samples with temperature seems to show slight deviation from Arrhenius behaviour. Thus the ion conduction mechanism might involve both ion hopping mechanism and segmental motion of the polymer chain segments. Jeon et al.⁽²⁵⁾, explained that with increase in temperature, more free volume is produced. As a result of increase in the degree of freedom of polymer chain segments of the electrolyte the ions, solvated molecules or the polymer chain

segments can move into the free volume easily which leads to enhancement of the ionic conductivity. In other words, the non-linearity indicates that ion transport in polymer electrolytes follows VTF relation. The temperature dependence of ionic conductivity suggests that the ion moves through the plasticizer-rich phase. Because the conducting medium i.e. plasticizer rich phase involves the plasticizers ethylene carbonate and propylene carbonate, the nano-filler SiO₂, poly(methylmethacrylate) and poly(styrene-co-acrylonitrile), the characteristics of the viscous matrix are to be considered for deviation from Arrhenius behaviour⁽²⁶⁾.

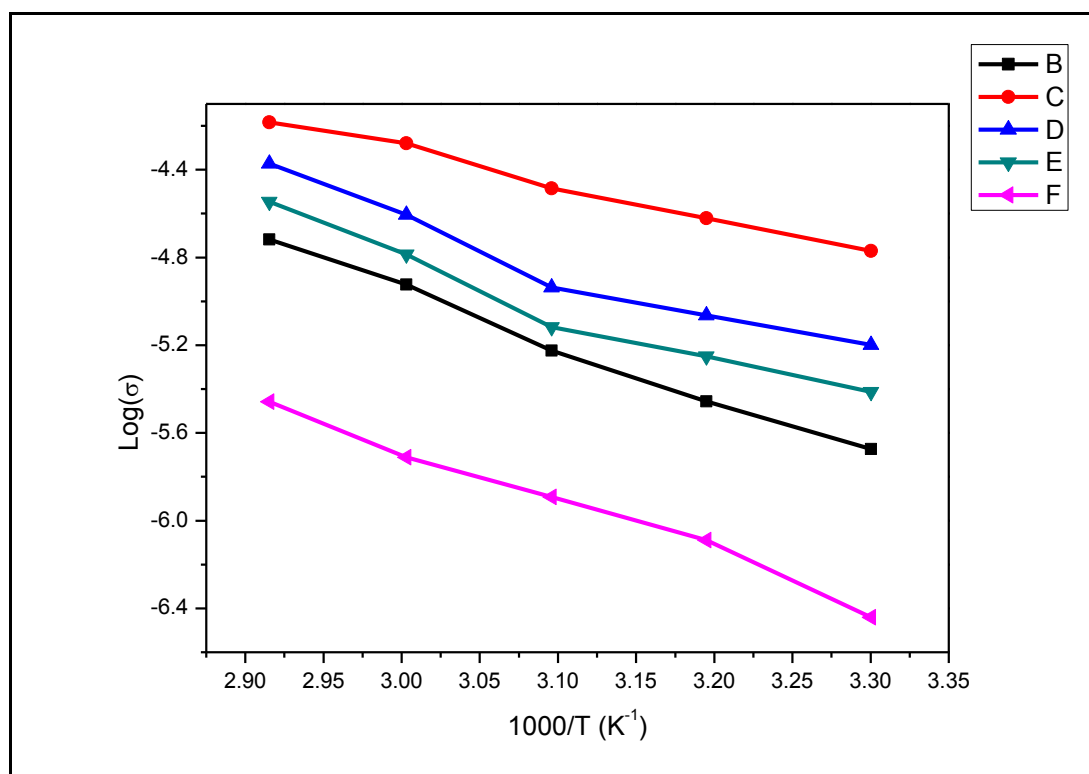


Figure 3.c. Arrhenius Plot for different concentration of nano-SiO₂ filler in SPE PMMA-PSAN-EC-PC-LiCF₃SO₃ were B=5 wt% SiO₂, C=6 wt% SiO₂, D=7 wt% SiO₂, E=8 wt% SiO₂, F=9 wt% SiO₂,

Table 2: Variation of ionic conductivity of solid polymer electrolytes at different concentration in (wt%) of nano-filler SiO₂ at different temperatures.

#	Sample	PMMA	PSAN	EC	PC	LiCF ₃ SO ₃	SiO ₂	$\sigma \times 10^{-05}$ (S cm ⁻¹)				
		wt%	wt%	wt%	wt%	wt%	wt%	30 °C	40 °C	50 °C	60 °C	70 °C
1	S0	25	25	15	15	20	0	0.147	0.209	0.502	0.925	1.876
2	S1	25	25	12.5	12.5	20	5	0.212	0.349	0.595	1.190	1.920
3	S2	25	25	12	12	20	6	1.700	2.390	3.270	5.260	6.550
4	S3	25	25	11.5	11.5	20	7	0.633	0.863	1.160	2.480	4.250
5	S4	25	25	11	11	20	8	0.386	0.562	0.764	1.630	2.840
6	S5	25	25	10.5	10.5	20	9	0.036	0.082	0.128	0.194	0.349

Thermal Stability

Thermo-gravimetric (TGA) Analysis technique were used to study the thermal stability of the sample S2 showing maximum conductivity. Figure 4 shows TG and derivative TG (DTG) profile of sample S2. The initial weight loss of 9 % at 162 °C is attributed to the loss of solvent and moisture. The gradual weight loss of 4 % until the samples reach 278 °C show the loss of trace amount of solvent impurities present in the sample. Beyond 278 °C, the weight loss up to 53% at 422 °C is attributed to the loss of plasticizers and polymer blend. The degradation of the triflate salt takes place beyond 422 °C until 497 °C amounting to 16%⁽²⁷⁾. The residue consisting of nano-filler SiO₂ and the carbon amounting to 13% is left behind at 650 °C⁽⁵⁾. The analysis shows that the sample S2 is thermally stable (up to 278 °C)⁽²⁸⁾. DTG graph shows maximum degradation of the

sample S2 at 387 °C and minor weight loss at 462 °C. It indicates the degradation of the polymer blend and its components as reported by TG analysis ^(29, 30).

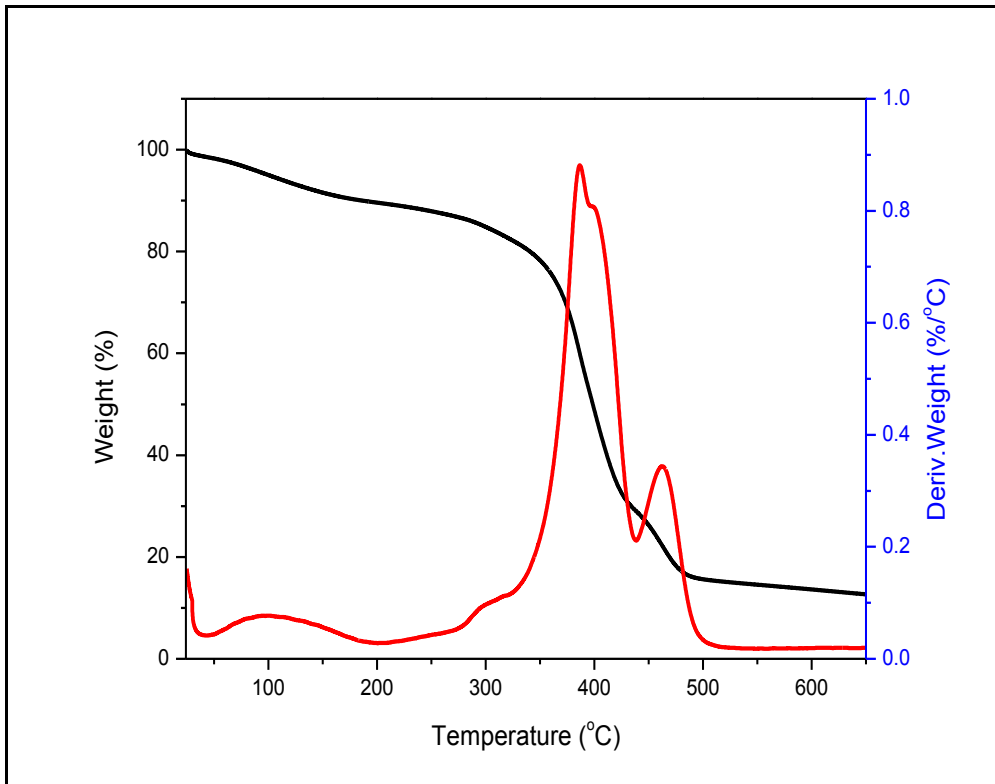


Figure 4: TG/DTG curves of SPE (S2)

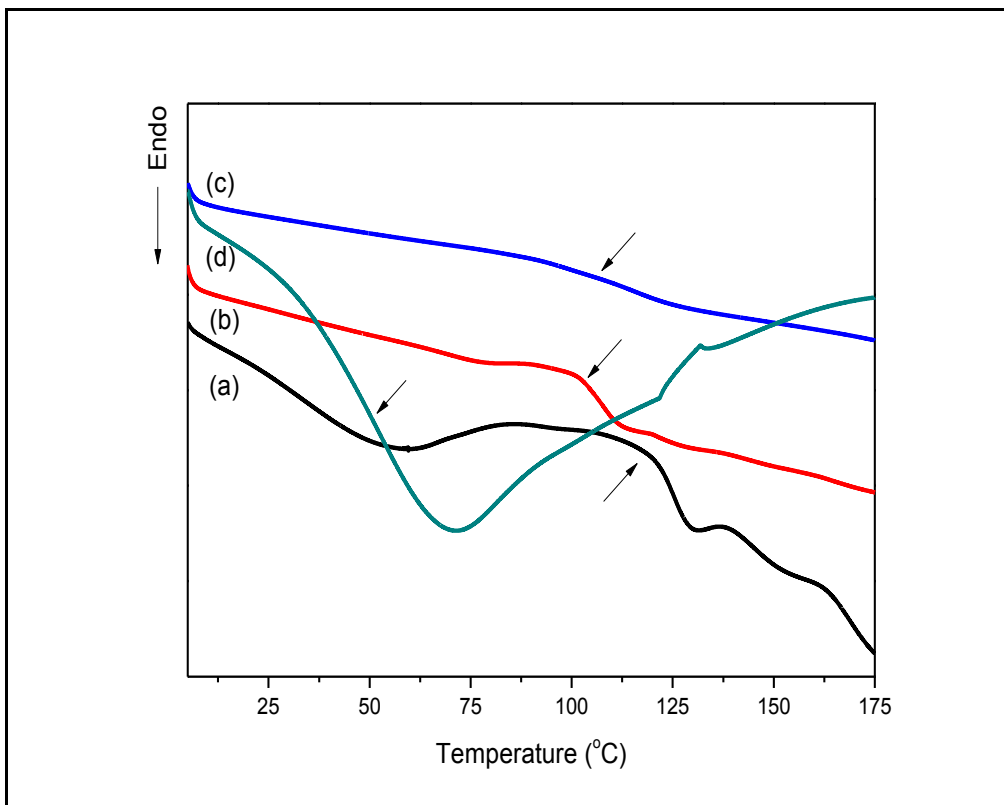
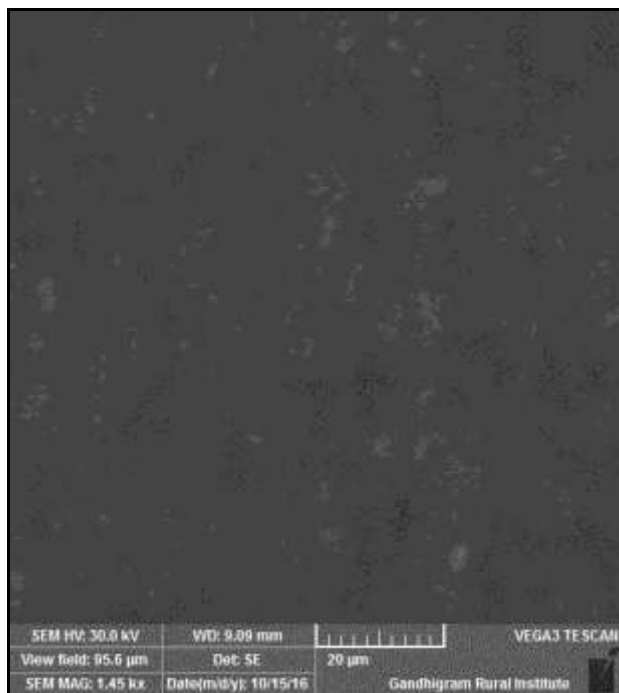


Figure 5: Differential scanning calorimetry curves for (a) pure PMMA, (b) pure PSAN, (c) SPE (S0), (d) SPE (S2).

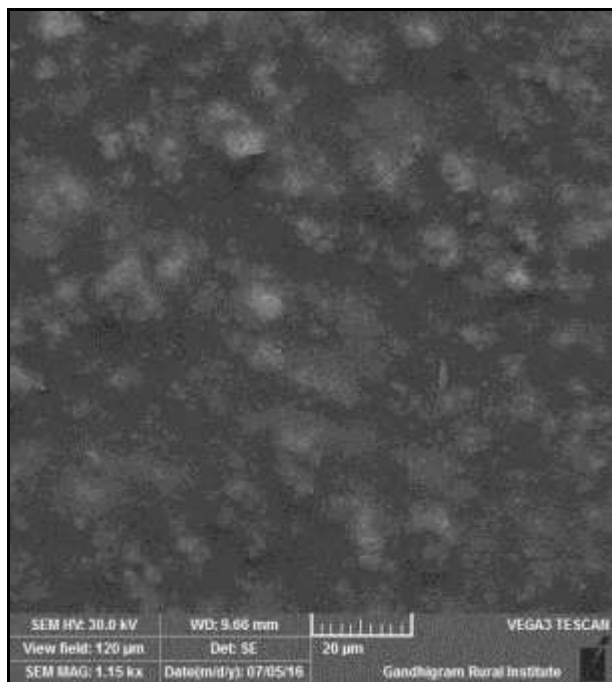
The DSC thermogram of pure PMMA, pure PSAN, S0 and S2 are shown in Fig. 5. The influence of each component and nanofiller SiO₂ on the glass transition temperature is studied. This study throws light on the phase transitions and physical changes in the solid polymer electrolytes upon influenced by temperature rise. The DSC studies coupled with thermo-gravimetric Analysis give overall picture on the thermal stability of the composite solid polymer electrolyte and its application in a particular temperature window⁽³¹⁾. DSC Analysis provides the T_g values of pure PMMA and PSAN at 120 °C and 100 °C respectively. Addition of plasticizers EC and PC into the above system involving PMMA, PSAN and Lithium triflate leads to complete miscibility and thus exhibits only one T_g value at 107.3 °C⁽³²⁾. This shows that the plasticizers help to solvate the lithium ions and make it miscible with polymer blend system by providing more amorphous rich phase⁽²⁸⁾. In the presence of nano filler SiO₂ (6 wt %) the above SPE exhibits T_g value at 50.4 °C. The drastic reduction of the T_g value shows the interaction of SiO₂ with polymer blend and the salt. This creates more amorphous rich phase with increased free volume around the polymer segments. Thus the polymers segments undergo increased segmental motion leading to increasing ion mobility as supported by the conductivity studies.

Morphology Studies

The Scanning electron microscopy images of the solid polymer electrolyte samples exhibiting highest conductivity (S2) and lowest conductivity (S5) are shown in the Fig. 6. From the figure, SEM micrograph of sample (S5) with 9 wt% of SiO₂ nano-filler shows irregular surface containing coagulates of the filler and lithium salt. The high density of coagulates hinder mobility of the ion and thus lowers ionic conductivity. The sample (S2) with 6 wt% of SiO₂ nano-filler shows surface morphology in which the nano-filler SiO₂ has blend with the polymer electrolyte and created more channels for ionic migration. Thus increases ionic mobility and hence ionic conductivity.



SPE (S2)



SPE (S5)

Figure 6: Scanning electron microscope image of polymer electrolyte samples S2 and S5. The samples were recorded at 30 KV. Magnification factor for sample S2 is 1450 and for sample S5 is 1150 respectively.

Conclusion

Poly(methyl methacrylate) and poly(styrene-co-acrylonitrile) based solid polymer electrolyte involving plasticizers ethylene carbonate and propylene carbonate with Lithium triflate as a salt and varying concentration of nano filler SiO₂ is prepared by solution casting technique using solvent tetrahydrofuran. The absence of XRD peaks characteristic of Lithium triflate salt and SiO₂ nano filler in sample S2 reveal that both the salt and filler are blend by the system and are involved in interactions with the polymer blend system. From XRD studies, it can be inferred that amorphous nature of the system supports increase in ionic conductivity. The ionic conductivity study reveals that solid polymer electrolyte sample S2 with 6 wt% of nanofiller SiO₂ shows maximum conductivity of $6.55 \times 10^{-5} \text{ S cm}^{-1}$ at 70 °C. The temperature dependence of ionic conductivity follows VTF relation. The interaction of C=O and –OCH₃ groups of PMMA with Li⁺ ion and the complexation of the blend polymer with the lithium salt were studied by FT-IR spectroscopy. The addition of nano-filler SiO₂ interacts with Lithium ion and the polymer segments increasing the ionic mobility and prevents formation of ion-ion doublets and multiplets. TG/DTG analysis reveals the thermal stability of highest conducting solid polymer electrolyte sample S2 up to 278 °C with maximum degradation at 387 °C and 462 °C. DSC studies reveal reduction in glass transition temperature T_g for SPE when compared with individual polymers and their blend. This shows the effectiveness of nano-filler SiO₂ in enhancing the conductivity and thermal stability of the polymer electrolyte sample. Morphological studies using SEM micrographs reveals that incorporation of nano-filler SiO₂ (at 6 wt %) shows formation of ion-conducting channels leading to enhancement of ionic conductivity. Further work involving different fillers and lithium salts on enhancement of conductivity and thermal stability to the polymer blend system involving PMMA and PSAN is currently undergoing in our research lab.

References:

1. Noto VD, Lavina S, Giffin GA, Negro E, Scrosati B, *Electrochim Acta* (2011) 57:4-13.
2. Quartarone E, Mustarelli P, *Chem Soc Rev* (2011) 40:2525-2540.
3. Agrawal RC, Pandey GP, *J Phys D Appl. Phys* (2008) 41:223001.
4. Stephan AM, *Eur Polym J* (2006) 42:21–42.

5. Rajeswari N, Selvasekarapandian S, Prabu M, Karthikeyan S, Sanjeeviraja C, Bull Mater Sci (2013) 36(2):333-339.
6. Rajendran S, Sivakumar M, Subadevi R, Mater Lett (2004) 58:641-649.
7. Shahzada Ahmad, Sharif Ahmad, S. A. Agnihotry, Ionics (2004) 10(3):268-272.
8. S. Ramesh, Liew Chiam Wen, Ionics (2010) 16:255-262.
9. Kumaraswamy GN, Ranganathaiah C, Deepa Urs MV, Ravikumar HB, Eur Polym J (2006) 42:2655-2666.
10. Miao D, Jianhua G, Qiang Z., Polymer (2004) 45:6725-6730.
11. L. Othman, K. W. Chew, Z. Osman, Ionics, (2007), 13(5): 337-342
12. Ramesh S, Leen KH, Kumutha K, Arof AK, Spectrochim Acta Part A(2007) 66:1237-1242.
13. Helan Flora X, Ulaganathan M, Shanker Babu R, Rajendran S, Ionics (2012) 18:731-736.
14. Rajendran S, Mahendran O, Mahalingam T, Eur Polym J (2002) 38(1):49-55.
15. Su'ait MS, Ahmad A, Hamzah H, Rahman MYA, Electrochim. Acta (2011) 57:123-131.
16. Rajendran S, Kannan R, Mahendran O., Mater Lett (2001) 49:172-179.
17. Pradhan DK, Choudhary RNP, Samantaray BK, Int J Electrochem Sci (2008) 3:597- 608.
18. Chew KW, Tan KW, Int J Electrochem Sci (2011) 6:5792 - 5801.
19. TianKhoon L, Ataollahi N, Hassan NH, Ahmad A, J Solid State Electrochem (2016) 20:203-213.
20. Jacob MME, Prabakaran SRS, Radhakrishna S, Solid State Ionics (1997) 104:267-276.
21. Kim C, Lee G, Lio K, Rhu KS, Kang OSG, Chang SH, Solid State Ionics (1999) 123:251-257.
22. Rajendran S, Mahendran O, Krishnaveni K, J New Mat Electrochem Sys (2003) 6:25-28.
23. Hyung SK, Kyong SK, Won-II C, Byung WC, Hee WR, J Power Sources (2003) 124: 221-224.
24. Dissanayake MAKL, Jayathilaka PARD, Bokalawala RSP, Albinsson I, Mellander BE, J Power Sources (2003)119:409-414.
25. Jeon JD, Kwak SY, Cho BW, J Electrochem Soc (2005) 152:1583-1589.
26. Rajendran S, Uma T, Bull Mater Sci (2000) 23(1):31-34.
27. Reza Younesi, Gabriel M. Veith, Patrik Johansson, Kristina Edstrom, Tejs Vegge, Energy Environ. Sci. (2015) 8:1905-1922.
28. Prasanth R, Aravindan V, Srinivasan M, J Power Sources (2012) 202:299-307.
29. Vijayaraj M, Gopinath C S, Journal of Catalysis (2006) 243:376-388.
30. Gnanakumar E S, Gowda R R, Kunjir Shrikant, Ajithkumar T G, Rajamohanan P R, Chakraborty Debashis, and Gopinath C S, ACS Catalysis (2013) 3:303-311
31. S. Ramesh, K. C. Wong, Ionics (2009) 15(2):249-254.
32. Song JM, Kang HR, Kim SW, Lee WM, Kim HT, Electrochim Acta (2003) 48:1339-1346.
